Experimental and Modeling Investigation of the Temperature Activation of TDDB in Galvanic Isolators Based on Polymeric Dielectrics

Jurij L. Mazzola, *Graduate Student Member, IEEE*, Matteo Greatti, *Graduate Student Member, IEEE*, Christian Monzio Compagnoni, *Senior Member, IEEE*, Alessandro S. Spinelli, *Senior Member, IEEE*, Dario Paci, Fabrizio Speroni, Vincenzo Marano, Michele Lauria, and Gerardo Malavena, *Member, IEEE*

***Abstract*—We report experimental evidence revealing a nonmonotonic temperature dependence of time-dependent dielectric breakdown (TDDB) in galvanic isolators based on polymeric dielectrics. In particular, the lifetime of the device under TDDB stress decreases when temperature rises from room temperature (RT) to 100 °C and then steeply increases above the latter temperature. This effect, which introduces a turnaround in the Arrhenius plot of device lifetime, is explained as a result of two competing processes leading to the weakening and strengthening of polymeric chains in the dielectric material, respectively. The proposed physical picture is further supported by a simple numerical model that allows to investigate the temperature dependence of TDDB in galvanic isolators based on polymeric dielectrics under various working conditions.**

***Index Terms*—Galvanic isolators, moisture, polymeric dielectrics, semiconductor device modeling, semiconductor device reliability, time-dependent dielectric breakdown.**

I. Introduction

THANKS to their cost effectiveness, power efficiency, high performance, and high reliability, modern galvanic isolators are increasingly replacing optocouplers to allow the safe interaction between the low-voltage and the high-voltage parts of an electronic system [1], [2], [3]. Among the possible design options for galvanic isolators, those based on thick-dielectric capacitors or transformers integrated in the back end of line (BEOL) stage of a semiconductor process flow are the most profitable and energy efficient [2], [3], [4], [5]. In order to withstand stress voltages in the tens-of-kV range, the employed dielectric layer must be in the tens-of-micrometer range and offer high dielectric strength. To meet these demands, polymeric dielectrics are currently under intensive investigation for next-generation galvanic isolators [6], [7], [8], [9], [10], [11]. Some polymeric dielectrics such as polyimide (PI) and polybenzoxazole (PBO), in fact, have been explored for the BEOL stage of some microelectronic processes [12], [13], [14] and may offer a consolidated integration scheme along with relatively high dielectric strength in the hundreds-of-volts per micrometer range. However, the reliability of galvanic isolators based on these materials is yet to be fully explored and understood, starting from their time-dependent dielectric breakdown (TDDB) phenomenology and dependences.

In this work, extending our preliminary work in [15], we experimentally investigate the temperature activation of TDDB in thick-PBO capacitors that are at the basis of next-generation galvanic isolators. We provide clear evidence of a turnaround in the Arrhenius plot of device lifetime and explain the observed phenomenology in terms of the combined effect of two physical processes making the rupture of polymeric chains due to electrical stress more and less likely, respectively. Starting from the experimental evidence of a markedly different temperature activation for those two processes, we develop a numerical model to support our physical picture and explore the impact of temperature on TDDB under different stress conditions. Results highlight important aspects that can affect the reliability of next-generation galvanic isolators based on polymeric dielectrics.

II. Experimental TDDB Results

A. Samples and Setup

Fig. 1(a) shows the experimental samples investigated in this work and the setup used to study the temperature dependence of their TDDB lifetime. Test structures consist in metal/PBO/n^+silicon capacitors encapsulated in a package made of epoxy resin. A circular top electrode with diameter equal to 1 mm was adopted to define the device area (A). The PBO thickness (h) was limited to 7 μm to reach device breakdown over an experimental timescale of few weeks with a voltage limit that safely prevents arching and discharge phenomena during the test. Besides, the chosen voltage also avoids any possible impact on the results of the sockets and chipboards used to connect the samples under test to the measurement instruments. Applied electric field was close to

Manuscript received 22 November 2023; revised 8 April 2024 and 29 April 2024; accepted 15 May 2024. Date of publication 21 May 2024; date of current version 14 October 2024. *(Corresponding author: Gerardo Malavena.)*

Jurij L. Mazzola, Matteo Greatti, Christian Monzio Compagnoni, Alessandro S. Spinelli, and Gerardo Malavena are with the Dipartimento di Elettronica, Informazione e Bioingegneria, Politecnico di Milan, 20133 Milan, Italy (e-mail: gerardo.malavena@polimi.it).

Dario Paci and Fabrizio Speroni are with the Process Research and Development, STMicroelectronics, 20007 Cornaredo, Italy.

Vincenzo Marano and Michele Lauria are with Process Research and Development STMicroelectronics, 20864 Agrate Brianza, Italy.

Color versions of one or more figures in this article are available at https://doi.org/10.1109/TDEI.2024.3403528.

Digital Object Identifier 10.1109/TDEI.2024.3403528

© 2024 The Authors. This work is licensed under a Creative Commons Attribution 4.0 License.
For more information, see https://creativecommons.org/licenses/by/4.0/

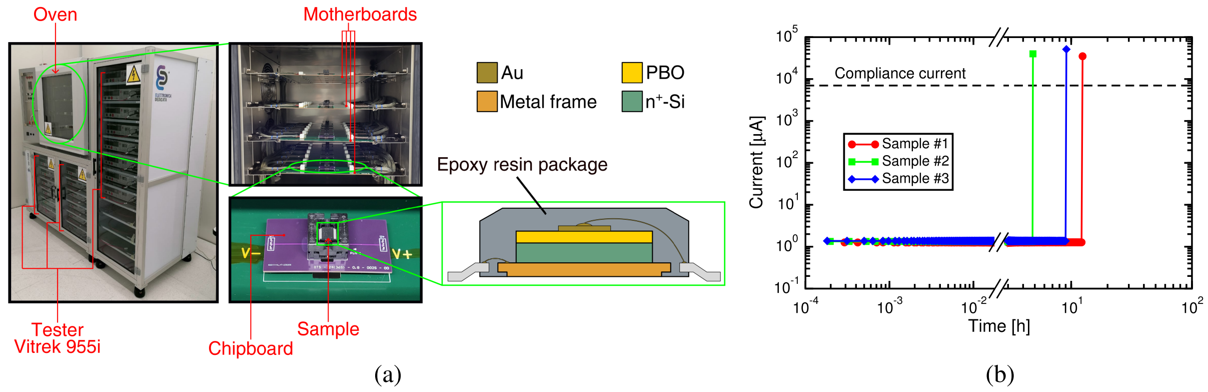

Fig. 1. (a) Schematic description of the experimental setup and of the samples investigated in this work. (b) Representative examples for the TDDB dynamics in the investigated samples (T_a = RT). On the y-axis, the rms value of the current is shown.

the typical dielectric strength of polymeric dielectrics, that is some MV/cm. To gather statistical data, up to 20 samples were measured in parallel by mounting their chipboards on mother boards placed in an oven and connected to 20 Vitrek 955i high-voltage testers. Each tester applies a 50-Hz sine stress voltage waveform to the top electrode of a sample and monitors the current through its bottom electrode. Sample breakdown is detected as a steep rise of its current above a compliance value equal to 7 mA. When that occurs, the duration of the stress time on the sample is stored as device lifetime in the TDDB test, and the electrical stress on the sample is interrupted. It is important to point out that the breakdown of a sample does not impact the electrical stress on the other samples tested in parallel, which proceeds unaffected.

B. Temperature Activation of TDDB

An example of the TDDB dynamics of the investigated samples is reported in Fig. 1(b). Data refer to the case of ambient temperature (T_a) equal to room temperature (RT) but are representative of all the explored stress conditions addressed in this work. The current flowing through the sample under test stays flat to the root-mean-square (rms) floor set by the charging/discharging of the metal/PBO/n$^+$silicon capacitor up to the breakdown event, which corresponds to the steep increase of the current above the compliance limit. In this regard, it is worth pointing out that, even with the minimum sampling interval of 60 ms made available by the high-voltage tester, no current data points have ever been detected in our experiments in-between the floor level and the compliance level as a result of device breakdown. That suggests that the breakdown process is an extremely abrupt phenomenon in the investigated devices, in agreement with what typically observed in thick-dielectric capacitors with metal electrodes [16], [17], [18], [19].

Fig. 2 shows the cumulative distribution of device lifetime gathered at different T_a ranging from RT to 115 °C. Data reveal a weak leftward shift of the distribution when T_a is increased from RT to 100 °C and a strong rightward shift of the curve for higher temperatures. It is worth pointing out that the latter rightward shift is so strong that in the case of T_a = 115 °C, only one sample reached breakdown over the maximum explored stress time of three weeks. Dashed lines in Fig. 2 are guide for the eye to indicate that device lifetime exceeds the limit of experimental observation.

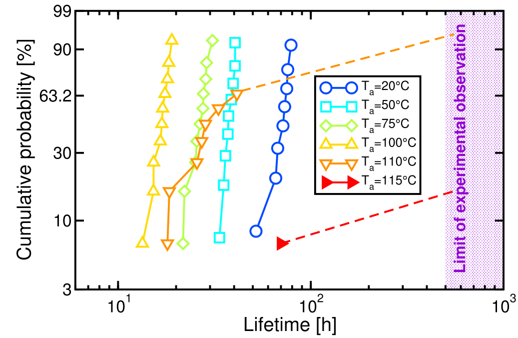

Fig. 2. Cumulative probability distribution of device lifetime at different T_a values. A Weibull representation has been used in the plot. Dashed lines indicate that device lifetime exceeds the limit of experimental observation.

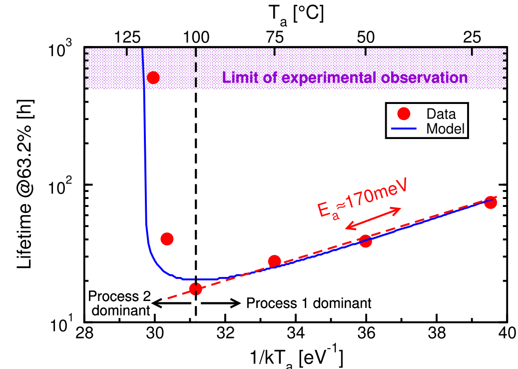

Fig. 3. Arrhenius plot for device lifetime at a cumulative probability of 63.2%, as resulting from the data reported in Fig. 2. The data point corresponding to T_a = 115 °C is representative of the fact that device lifetime is beyond the limit of experimental observation. See Section III-B and Fig. 9 for a description of Process 1 and Process 2.

To better highlight the TDDB temperature dependence of the samples, device lifetime at a probability of 63.2% (corresponding to the scale parameter of a Weibull statistics) was extracted from the cumulative distributions and used to build the Arrhenius plot shown in Fig. 3. The figure reveals not only that the increase in T_a from RT to 100 °C gives rise to a weak reduction of device lifetime but also that the data points in that temperature range are very well aligned over a straight line corresponding to an activation energy $E_a \approx 170$ meV. Increasing T_a above 100 °C, instead, makes clearly evident a turnaround in the Arrhenius plot and a steep growth of device

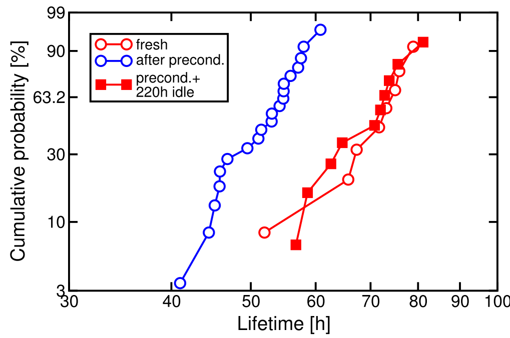

Fig. 4. Device lifetime distributions showing the impact of a high-humidity preconditioning on TDDB. The red curve with square markers was gathered by inserting a 220 h idle time between the end of the preconditioning and the start of the electrical stress phase.

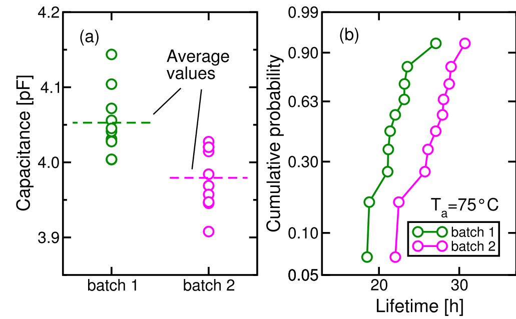

Fig. 5. (a) Comparison between capacitance values measured on two batches of samples that differ in their average moisture content. (b) TDDB lifetime distributions gathered on samples of the batches of (a).

lifetime. Similar results (not reported here for brevity) were obtained on similar metal/PI/n$^+$silicon capacitors.

C. Impact of Moisture on TDDB

It is widely accepted that the moisture content in polymers affects their dielectric strength [13], [20], [21], [22]. This suggests that even the TDDB dynamics of these materials may be impacted by their moisture content. To demonstrate this point on our samples and check the possible impact of moisture on the results presented in Section II-B, we performed some ad hoc TDDB tests. In the first one, we preconditioned a batch of samples for 192 h at $T_a = 30$ °C and relative humidity (RH) equal to 60% before measuring their TDDB lifetime distribution at RT. The comparison between the resulting device lifetime distribution and that previously gathered on fresh samples tested under the same stress conditions is shown in Fig. 4. Results reveal that the distribution of the preconditioned samples is shifted leftwards with respect to that of fresh samples, with the statistical spread of device lifetime practically unaffected by the preconditioning phase. To understand whether the previous effect is either permanent or transient, we repeated the preconditioning on a further batch of samples but waited 220 h under normal T_a/RH conditions of our laboratory before the electrical stress phase. Fig. 4 shows that the impact of the preconditioning phase on TDDB lifetime vanishes due to the idle time and that the resulting distribution is practically equal to that of fresh samples. The previous evidence seems to suggest that the decrease in device lifetime due to preconditioning can be simply related to moisture absorption from the ambient while the opposite process takes place during the idle time between the end of the preconditioning and the start of the electrical stress phase. The observed phenomenology seems to agree with results reported in [20], which show that dielectric degradation due to hydrolysis processes is completely recovered by baking the dielectric after the high-humidity treatment.

Along with the decrease in device lifetime discussed so far, another electrical property of polymeric dielectrics that can change due to moisture absorption is relative permittivity [23], [24]. The high polarizability of water molecules inside the dielectric, in fact, can contribute to increasing the dielectric constant of the material and, as a consequence, the capacitance of our devices. The previous fact suggests the possibility to exploit capacitance measurements to monitor the moisture content in our devices and understand how the latter is related to device lifetime. Fig. 5 relates the capacitance values measured on two batches of devices that differ in their moisture concentration with the TDDB lifetime distributions of the same batches. Data clearly show that the lifetime distribution of samples with a higher average capacitance (hence, higher moisture concentration) is shifted leftwards with respect to that of the remaining samples. Interestingly, the previous evidence allows to exploit device capacitance measurements to investigate moisture absorption and desorption dynamics to relate them to the temperature activation of TDDB lifetime.

III. Modeling

The nonmonotonic temperature dependence of TDDB can be considered as the outcome of the action of two competing processes. The first one is the degradation of the insulating properties of the polymeric dielectric due to the applied electrical stress. Such degradation is a consequence of the rupture of polymeric chains which can occur for various physical mechanisms [13], [25], [26], [27], [28] and eventually results in dielectric breakdown. A weak temperature dependence can be assumed for this process, compatible with the low activation energy reported for other degradation phenomena of dielectrics [28], [29], [30].

The second of the two processes that lead to the turnaround in the Arrhenius plot for $T_a > 100$ °C can be identified in the outdiffusion of water molecules. This outdiffusion should, in fact, be enhanced by the increase in T_a, making the dielectric less prone to breakdown and resulting in the increase in device lifetime. In Section III-A, we present a detailed experimental investigation of moisture outdiffusion dynamics and show that the time and temperature dependence of the results are quantitatively compatible with our proposed physical picture. Then, starting from the previous evidence, in Section III-B, we develop a numerical model that catches the main features of the T_a dependence of TDDB and the impact of moisture on the activation energy of the phenomenon.

A. Analysis of Moisture Outdiffusion Dynamics

In order to investigate the dynamics of moisture desorption from our samples, we performed the experimental scheme

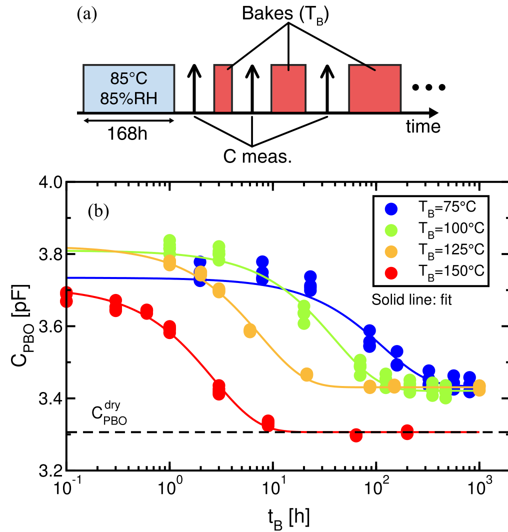

Fig. 6. (a) Schematic of the test scheme used to investigate the outdiffusion of moisture from our samples through capacitance measurements. (b) Results of the experiments made according to (a) showing the decrease in device capacitance due to moisture outdiffusion.

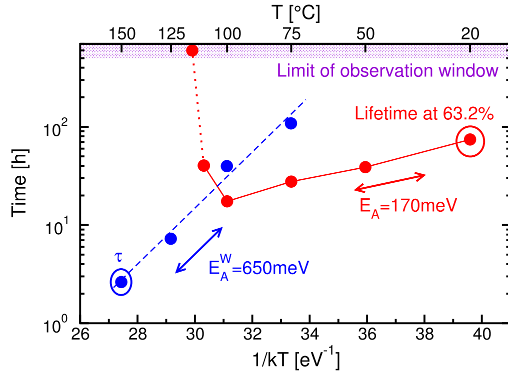

Fig. 7. Arrhenius plot of τ as extracted from the transients of Fig. 6 compared to the Arrhenius plot of device lifetime of Fig. 3.

in Fig. 6(a). First, we preconditioned our devices with a 168 h-long high-humidity treatment under controlled temperature and RH conditions equal to 85 °C and 85%, respectively. After that, we monitored the decrease in device capacitance (C_{PBO}) over high-temperature bake periods. During these periods, the devices were kept in an oven at temperature T_B but each capacitance readout was performed at RT after chip cooling. For each T_B, the experiment was made on six samples to highlight a possible statistical variability in the results. Fig. 6(b) reveals that C_{PBO} of all the samples decreases with time and that the process shows a strong acceleration with T_B. Besides, devices sharing the same T_B display a very similar behavior, meaning that the statistical variability in C_{PBO} does not impact the main features of the observed phenomenon. In particular, Fig. 6(b) also shows that the decrease in C_{PBO} over time can be reproduced by an exponential relation such as

$$C_{\mathrm{PBO}}(t) = C_{\mathrm{PBO}}^{\mathrm{final}} - \left[C_{\mathrm{PBO}}^{\mathrm{final}} - C_{\mathrm{PBO}}(0)\right]e^{-t_B/\tau}. \quad (1)$$

In the previous equation, t_B is the cumulative bake time, $C_{\mathrm{PBO}}^{\mathrm{final}}$ is the value taken by C_{PBO} when stationary conditions are reached after a sufficiently long t_B, and τ is the characteristic time constant of the exponential. Fig. 7 shows that τ changes with T_B according to an Arrhenius law with activation energy (E_A^W) equal to 650 meV. The results in Figs. 6 and 7 can be regarded as evidence of the desorption of water molecules from the polymeric dielectric over time and of its acceleration by T_B. Besides, the comparison between the Arrhenius plot of τ and that of device lifetime at 63.2% in Fig. 3 (reported again in Fig. 7 for clarity) reveals that the curves cross each other when T_B approaches 100 °C. In fact, even though τ is much longer than device lifetime at low temperatures, the relation between the two physical quantities becomes the opposite when temperature increases, due to the fact that $E_A^W > E_A$. Fig. 8 shows, moreover, that the previous moisture outdiffusion dynamics remain the same in the case of non-preconditioned samples. When the high-humidity treatment is not present, in fact, the overall variation of device capacitance during the bake phase in Fig. 8 is smaller than that in Fig. 6(b) but, nevertheless, both data follow an exponential trend with the same time constant.

From a physical standpoint, all the previous results indicate that when $T_{\mathrm{a}} < 100$ °C device breakdown occurs before any relevant changes in the moisture content of the dielectric. On the other hand, when $T_{\mathrm{a}} > 100$ °C, the fact that water molecules diffuse out of the material before breakdown occurs leads to the increase in device lifetime. It is worth mentioning that the T_{a} value corresponding to the turnaround in the Arrhenius plot of device lifetime is the outcome of the interplay between dielectric degradation dynamics and moisture outdiffusion which, in general, depend not only on the electrical stress conditions but also on device and package properties. The fact that the previous T_{a} value is close to 100 °C must not be intended as an inherent property of all polymeric materials, rather as the outcome of the chosen test conditions and geometric and physical parameters of the investigated devices.

For a quantitative description of the previous process, the density of water molecules (n_w) can be obtained from the following formula [31]:

$$n_w = \frac{\rho_w N_A}{m_w} \frac{\left(\varepsilon_{\mathrm{PBO}} - \varepsilon_{\mathrm{PBO}}^{\mathrm{dry}}\right)\left(\varepsilon_w + 3\varepsilon_{\mathrm{PBO}}^{\mathrm{dry}}\right)}{\left(\varepsilon_{\mathrm{PBO}} + 3\varepsilon_{\mathrm{PBO}}^{\mathrm{dry}}\right)\left(\varepsilon_w - \varepsilon_{\mathrm{PBO}}^{\mathrm{dry}}\right)} \quad (2)$$

where $\varepsilon_{\mathrm{PBO}}^{\mathrm{dry}}$ and ε_w are the relative dielectric constants of PBO with no moisture inside and of water, respectively, $\varepsilon_{\mathrm{PBO}}$ is the relative dielectric constant of PBO filled with a uniform concentration of water molecules equal to n_w, ρ_w is the specific weight of water, N_A is the Avogadro constant, and m_w is the molar mass of water. In the previous equation, $\varepsilon_w = 80$ was assumed, and $\varepsilon_{\mathrm{PBO}}$ and $\varepsilon_{\mathrm{PBO}}^{\mathrm{dry}}$ were computed from the sample capacitance in the nondry and dry conditions as $(C_{\mathrm{PBO}}h)/(\varepsilon_0 A)$ and $(C_{\mathrm{PBO}}^{\mathrm{dry}}h)/(\varepsilon_0 A)$, respectively ($\varepsilon_0$ is the vacuum permittivity). In particular, $C_{\mathrm{PBO}}^{\mathrm{dry}}$ was assumed equal to the lower capacitance among those that were measured in Fig. 6, corresponding to $C_{\mathrm{PBO}}^{\mathrm{final}}$ of the experiment at $T_B =$ 150 °C (black dashed line).

Considering that the decrease in C_{PBO} in Fig. 8 due to moisture outdiffusion is small with respect to the value of

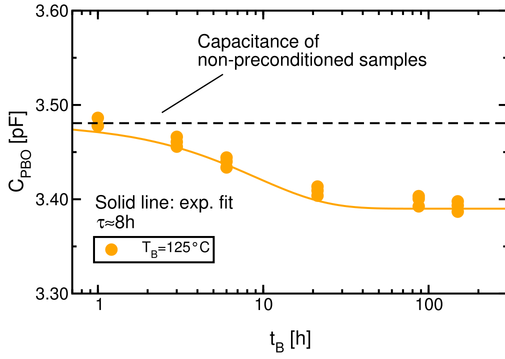

Fig. 8. Results of experiments similar to those of Fig. 6 but without the initial high-humidity treatment. The value of τ used in the exponential fit was taken from the Arrhenius plot of Fig. 6.

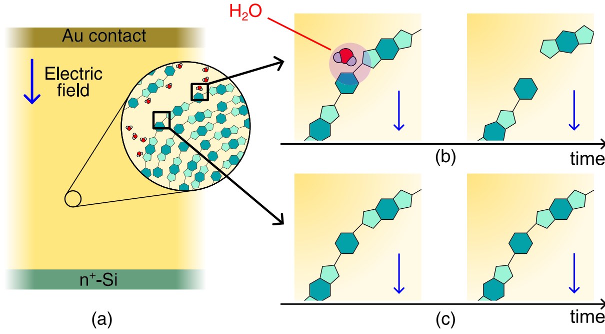

Fig. 9. Schematic description of the physical picture proposed to explain the turnaround in the Arrhenius plot of Fig. 3.

C_{PBO} of fresh samples ($C_{\text{PBO}}^{\text{fresh}}$), (2) can be approximated as

$$n_w \approx n_w^{\text{fresh}} + K\left(\varepsilon_{\text{PBO}} - \varepsilon_{\text{PBO}}^{\text{fresh}}\right) \tag{3}$$

with

$$K = \frac{\rho_w N_A}{m_w} \frac{4\varepsilon_{\text{PBO}}^{\text{dry}}}{(3\varepsilon_{\text{PBO}}^{\text{dry}} + \varepsilon_{\text{PBO}}^{\text{fresh}})^2} \frac{\varepsilon_{\text{PBO}} + 3\varepsilon_{\text{PBO}}^{\text{dry}}}{\varepsilon_w - \varepsilon_{\text{PBO}}^{\text{dry}}} \tag{4}$$

where $\varepsilon_{\text{PBO}}^{\text{fresh}} = (C_{\text{PBO}}^{\text{fresh}} h)/(\varepsilon_0 A)$ and n_w^{fresh} is the concentration of water molecules computed with (2) when $\varepsilon_{\text{PBO}} = \varepsilon_{\text{PBO}}^{\text{fresh}}$. Thanks to the linear relation between ε_{PBO} and n_w in (3), the time evolution of n_w can be expressed with an exponential law with time constant equal to τ as in (1)

$$n_w(t) = n_w^{\text{final}} - \left[n_w^{\text{final}} - n_w(0)\right]e^{-t_B/\tau} \tag{5}$$

where all the symbols in the previous equation have the same meaning of the respective ones in (1).

B. Modeling Results for TDDB

We started from the idea suggested in [13] for polymeric dielectrics similar to ours and assumed that dielectric breakdown is the outcome of the generation of defect states resulting from the rupture of polymeric chains due to electrical stress. As a consequence, the degradation of the material can be described by the density of defect states (n_d), and dielectric breakdown occurs when n_d exceeds a threshold n_d^{th}. According to our proposed physical picture, however, the rupture of polymeric chains and the generation of new defect states can happen only when the reaction with water molecules is involved in the process. Despite being a sharp simplification of the actually involved physical mechanisms, the previous approach will be shown to be enough to catch the main features of the temperature dependence of TDDB. The proposed picture is schematically represented in Fig. 9, which shows that only the concurrent action of water molecules and electrical stress [Fig. 9(b)] leads to polymeric chains rupture, while the previous process is precluded by the absence of water molecules [Fig. 9(c)]. According to this picture, it is therefore possible to write

$$\frac{dn_d}{dt} = rn_w \tag{6}$$

where r is the defect generation rate. Considering that when n_w is constant, the temperature activation of n_d and of device lifetime is determined by r, and we assumed $r = r_0 e^{-E_A/kT_a}$, where r_0 is a prefactor, k is the Boltzmann's constant, and $E_A = 170$ meV is the activation energy extracted from the region of the curve in Fig. 3 that follows an Arrhenius-like trend. Integrating (6) with $n_d(0) = 0$, n_d can be computed as

$$n_d = r\int_0^t n_w d\eta. \tag{7}$$

To compute n_d from the previous equation, a further relation for the time evolution of n_w is needed. We considered that the concentration of water molecules in the material can decrease because of two mechanisms. The first is the outdiffusion of water molecules ruled by the gradient of concentration with the external ambient. The second mechanism, instead, consists in the disappearing of water molecules when they contribute to creating precursors for the generation of new defects. The rate of the former process can be computed assuming that moisture outdiffusion dynamics are not affected by the presence of electrical stress. Computing the time derivative of (5), the previous rate results in $-(n_w - n_w^{\text{final}})/\tau$. The rate of the latter process, instead, coincides with the defect generation rate expressed in (6). As a consequence, the complete rate equation for n_w reads

$$\frac{dn_w}{dt} = -(n_w - n_w^{\text{final}})/\tau - rn_w. \tag{8}$$

The previous equation can be solved for n_w with $n_w(0)$ computed from $C_{\text{PBO}}^{\text{fresh}}$ through (2). Given $n_w(t)$, $n_d(t)$ can be computed through (6) and, in turn, device lifetime as the time corresponding to the condition $n_d = n_d^{th}$.

Simulation results in terms of n_w and n_d are shown in Fig. 10. In particular, simulated device lifetime at different T_a values is also shown in Fig. 10(a) to easily relate the lifetime with n_w. Results confirm that n_w barely changes with respect to $n_w(0)$ when $T_a < 100$ °C and that the decrease in device lifetime with T_a comes from the temperature activation of r with $E_A = 170$ meV. The previous dynamics can be understood by noting that the curves in Fig. 10(b) shift leftwards when T_a increases in this regime, and the same happens also to the time at which $n_d = n_d^{th}$. However, since $E_A^W > E_A$, the previous condition does not hold anymore when T_a approaches 100 °C and n_w decreases significantly before the breakdown condition is met. In turn, the decrease in n_w slows down defect generation as can be seen in the inset

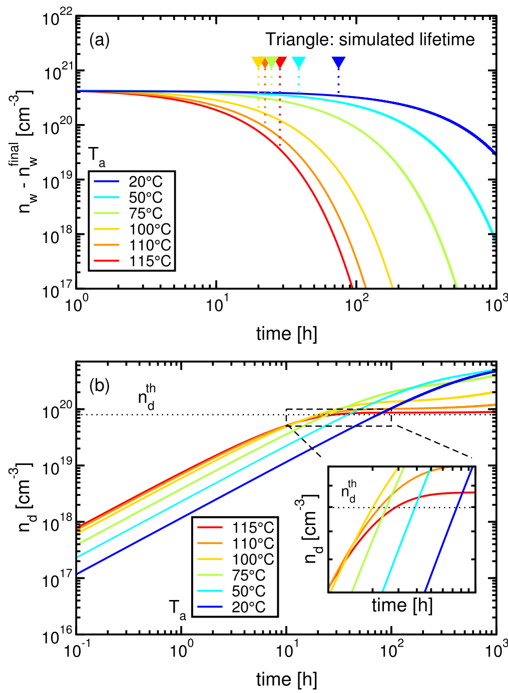

Fig. 10. (a) Simulation results showing n_w over time during electrical stress for different T_a values. (b) Simulation results showing n_d over time during electrical stress for different T_a values ($r_0 \approx 2.5$ h^{-1} was assumed).

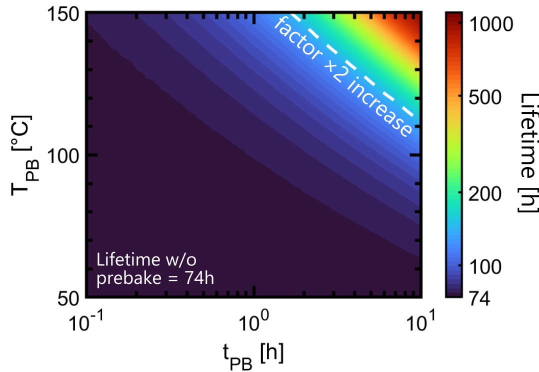

Fig. 11. Simulation results of the impact of a prebake preceding the electrical stress phase on device lifetime. The stress conditions were the same of those experimentally investigated in Fig. 2 with $T_a = 20$ °C.

of Fig. 10(b) and, eventually, delays device lifetime. Overall, the developed model can nicely reproduce the experimental evidence for device lifetime reported in Fig. 3 with only a limited number of free parameters, namely r_0 and n_d^{th}. All the remaining physical quantities involved in the model, in fact, were retrieved from the experimental results discussed in Sections II and III.

Due to its simplicity, the developed model can be employed for a quick assessment of the impact of high-temperature phases on the performance of galvanic isolators based on polymeric dielectrics. For example, Fig. 11 shows the effect on fresh devices of a prebake of duration t_{PB} and at temperature T_{PB} before the electrical stress phase. The prebake conditions that lead to a particular increase in device lifetime (a factor 2 was chosen in the figure just a reference) can be easily extracted from the color map resulting from simulations.

IV. Conclusion

We have provided clear experimental evidence that the nonmonotonic temperature dependence of TDDB in galvanic isolators based on polymeric dielectrics can be explained as the outcome of two competing mechanisms: 1) the electrical degradation of the polymeric dielectric and 2) the outdiffusion of water molecules from the material during the electrical stress phase. Starting from the previous physical picture, we also developed a numerical model that easily allows to investigate important aspects of the reliability of galvanic isolators when operating under various ambient conditions.

References

[1] B. Chen, J. Wynne, and R. Kliger, "High speed digital isolators using microscale on-chip transformers," *Elektronik Mag.*, vol. 15, pp. 1–6, Jul. 2003.

[2] B. Chen and S. Diaham, "Polyimide films for digital isolators," in *Polyimide for Electronic and Electrical Engineering Applications*. London, U.K.: InTechOpen, 2020, ch. 6, doi: 10.5772/intechopen.93343.

[3] E. Ragonese, G. Palmisano, A. Parisi, and N. Spina, "Highly integrated galvanically isolated systems for data/power transfer," in *Proc. 26th IEEE Int. Conf. Electron., Circuits Syst. (ICECS)*, Nov. 2019, pp. 518–521, doi: 10.1109/ICECS46596.2019.8965151.

[4] E. Ragonese, N. Spina, A. Parisi, and G. Palmisano, "An experimental comparison of galvanically isolated DC–DC converters: Isolation technology and integration approach," *Electronics*, vol. 10, no. 10, p. 1186, May 2021, doi: 10.3390/electronics10101186.

[5] T. Bonifield, "Enabling high voltage signal isolation quality and reliability," Texas Instrum., Dallas, TX, USA, Tech. Rep., SSZY028, 2017, pp. 1–6.

[6] S. Diaham, S. Zelmat, M.-L. Locatelli, S. Dinculescu, M. Decup, and T. Lebey, "Dielectric breakdown of polyimide films: Area, thickness and temperature dependence," *IEEE Trans. Dielectr. Electr. Insul.*, vol. 17, no. 1, pp. 18–27, Feb. 2010, doi: 10.1109/TDEI.2010.5411997.

[7] S. Diaham et al., "Improving polyimide isolation performance by tailoring interfaces with nitride layers for digital isolator application," in *Proc. IEEE 3rd Int. Conf. Dielectrics (ICD)*, Jul. 2020, pp. 570–573, doi: 10.1109/ICD46958.2020.9341967.

[8] G. Malavena et al., "Investigation of the statistical spread of the time-dependent dielectric breakdown in polymeric dielectrics for galvanic isolation," in *Proc. IEEE Latin Amer. Electron Devices Conf. (LAEDC)*, Jul. 2022, pp. 1–4, doi: 10.1109/LAEDC54796.2022.9908226.

[9] T. Bonifield, H. Guo, J. West, H. Shichijo, and T. Tahir, "High frequency TDDB of reinforced isolation dielectric systems," in *Proc. IEEE Int. Rel. Phys. Symp. (IRPS)*, Apr. 2020, pp. 1–4, doi: 10.1109/IRPS45951.2020.9128352.

[10] L. Guinane et al., "Electric field DC conductivity dependency of polyimide films," *IEEE Trans. Dielectr. Electr. Insul.*, vol. 27, no. 5, pp. 1440–1445, Oct. 2020, doi: 10.1109/TDEI.2020.9215091.

[11] M. Salina, F. Cerini, L. Montagna, S. Adorno, D. Paci, and D. Asnaghi, "Polyimide-based integrated transformers and capacitors for high voltage galvanic isolation," in *Proc. IEEE 4th Int. Conf. Dielectrics (ICD)*, Jul. 2022, pp. 454–457, doi: 10.1109/ICD53806.2022.9863525.

[12] S. Palit and M. A. Alam, "Electrical breakdown in polymers for BEOL applications: Dielectric heating and humidity effects," in *Proc. IEEE Int. Rel. Phys. Symp.*, Jun. 2014, pp. 1–4, doi: 10.1109/IRPS.2014.6861114.

[13] S. Palit, D. Varghese, H. Guo, S. Krishnan, and M. A. Alam, "The role of dielectric heating and effects of ambient humidity in the electrical breakdown of polymer dielectrics," *IEEE Trans. Device Mater. Rel.*, vol. 15, no. 3, pp. 308–318, Sep. 2015, doi: 10.1109/TDMR.2015.2431998.

[14] S. Zelmat, M.-L. Locatelli, T. Lebey, and S. Diaham, "Investigations on high temperature polyimide potentialities for silicon carbide power device passivation," *Microelectronic Eng.*, vol. 83, no. 1, pp. 51–54, Jan. 2006, doi: 10.1016/j.mee.2005.10.050.

[15] J. L. Mazzola et al., “Modeling the temperature dependence of TDDB in galvanic isolators based on polymeric dielectrics,” in *Proc. IEEE 53rd Eur. Solid-State Device Res. Conf. (ESSDERC)*, Sep. 2023, pp. 160–163, doi: 10.1109/essderc59256.2023.10268573.

[16] M. Hikita, I. Kanno, G. Sawa, and M. Ieda, “Consideration on filamentary thermal breakdown by measuring pre-breakdown current in solid dielectrics,” *Jpn. J. Appl. Phys.*, vol. 24, no. 8, pp. 984–987, Aug. 1985, doi: 10.1143/jjap.24.984.

[17] M. Hikita, I. Kanno, G. Sawa, and M. Ieda, “Solid breakdown process from viewpoint of nature of pre-breakdown current in polymeric insulating materials,” *Jpn. J. Appl. Phys.*, vol. 24, no. 12, pp. 1619–1622, Dec. 1985, doi: 10.1143/jjap.24.1619.

[18] M. Hikita, T. Hirose, Y. Ito, T. Mizutani, and M. Ieda, “Investigation of electrical breakdown of polymeric insulating materials using a technique of pre-breakdown current measurements,” *J. Phys. D, Appl. Phys.*, vol. 23, no. 12, pp. 1515–1527, Dec. 1990, doi: 10.1088/0022-3727/23/12/007.

[19] T. Kauerauf et al., “Abrupt breakdown in dielectric/metal gate stacks: A potential reliability limitation?” *IEEE Electron Device Lett.*, vol. 26, no. 10, pp. 773–775, Oct. 2005, doi: 10.1109/LED.2005.856015.

[20] L. Li, N. Bowler, P. R. Hondred, and M. R. Kessler, “Statistical analysis of electrical breakdown behavior of polyimide following degrading processes,” *IEEE Trans. Dielectr. Electr. Insul.*, vol. 18, no. 6, pp. 1955–1962, Dec. 2011, doi: 10.1109/TDEI.2011.6118633.

[21] F. J. Campbell, A. K. Brewer, R. J. Orr, T. A. Janicke, and A. M. Bruning, “Hydrolytic deterioration of polyimide insulation on naval aircraft wiring,” in *Proc. IEEE Conf. Electr. Insul. Dielectr. Phenomena (CEIDP)*, Oct. 1988, pp. 180–188, doi: 10.1109/CEIDP.1988.26329.

[22] Y. Mecheri, M. Nedjar, A. Lamure, M. Aufray, and C. Drouet, “Influence of moisture on the electrical properties of XLPE insulation,” in *Proc. Annu. Rep. Conf. Electr. Insul. Dielectic Phenomena*, Oct. 2010, pp. 1–4, doi: 10.1109/CEIDP.2010.5724017.

[23] J. Melcher, Y. Deben, and G. Arlt, “Dielectric effects of moisture in polyimide,” *IEEE Trans. Electr. Insul.*, vol. 24, no. 1, pp. 31–38, Feb. 1989, doi: 10.1109/14.19863.

[24] P. J. Schubert and J. H. Nevin, “A polyimide-based capacitive humidity sensor,” *IEEE Trans. Electron Devices*, vol. ED-32, no. 7, pp. 1220–1223, Jul. 1985, doi: 10.1109/T-ED.1985.22104.

[25] K. Wu, L. A. Dissado, and T. Okamoto, “Percolation model for electrical breakdown in insulating polymers,” *Appl. Phys. Lett.*, vol. 85, no. 19, pp. 4454–4456, Nov. 2004, doi: 10.1063/1.1819526.

[26] K. Wu, Y. Wang, Y. Cheng, L. A. Dissado, and X. Liu, “Statistical behavior of electrical breakdown in insulating polymers,” *J. Appl. Phys.*, vol. 107, no. 6, Mar. 2010, Art. no. 064107, doi: 10.1063/1.3342468.

[27] L. A. Dissado, G. Mazzanti, and G. C. Montanari, “The role of trapped space charges in the electrical aging of insulating materials,” *IEEE Trans. Dielectr. Electr. Insul.*, vol. 4, no. 5, pp. 496–506, Oct. 1997, doi: 10.1109/94.625642.

[28] G. Mazzanti, G. C. Montanari, and L. A. Dissado, “A space-charge life model for AC electrical aging of polymers,” *IEEE Trans. Dielectr. Electr. Insul.*, vol. 6, no. 6, pp. 864–875, Dec. 1999, doi: 10.1109/94.822029.

[29] V. Huard, M. Denais, and C. Parthasarathy, “NBTI degradation: From physical mechanisms to modelling,” *Microelectron. Rel.*, vol. 46, no. 1, pp. 1–23, Jan. 2006, doi: 10.1016/j.microrel.2005.02.001.

[30] D. Resnati, G. Nicosia, G. M. Paolucci, A. Visconti, and C. Monzio Compagnoni, “Cycling-induced charge trapping/detrapping in Flash memories—Part I: Experimental evidence,” *IEEE Trans. Electron Devices*, vol. 63, no. 12, pp. 4753–4760, Dec. 2016, doi: 10.1109/TED.2016.2617888.

[31] X.-D. Liu et al., “A general model of dielectric constant for porous materials,” *Appl. Phys. Lett.*, vol. 108, no. 10, Mar. 2016, Art. no. 102902, doi: 10.1063/1.4943639.

Open Access funding provided by ‘Politecnico di Milano’ within the CRUI CARE Agreement